

Nonisothermal Melt Crystallization and Subsequent Melting Behavior of Biodegradable Poly(hydroxybutyrate)/Multiwalled Carbon Nanotubes Nanocomposites

CHANGLING XU, ZHAOBIN QIU

State Key Laboratory of Chemical Resource Engineering, Beijing University of Chemical Technology, Beijing 100029, China

Received 1 January 2009; revised 28 July 2009; accepted 29 July 2009

DOI: 10.1002/polb.21821

Published online in Wiley InterScience (www.interscience.wiley.com).

ABSTRACT: In this work, nonisothermal melt crystallization and subsequent melting behavior of poly(hydroxybutyrate) (PHB) and its nanocomposites at different multiwalled carbon nanotubes (MWCNTs) loadings were investigated. Increasing the MWCNTs loadings has enhanced the nonisothermal melt crystallization of PHB significantly in the nanocomposites when compared with that of the neat PHB; furthermore, increasing the cooling rates shift the crystallization exotherms to low temperature range for both neat PHB and its nanocomposites. Double melting behavior is found for both neat PHB and its nanocomposites crystallized nonisothermally from the melt, which is explained by the melting, recrystallization, and remelting model. Effects of the MWCNTs loadings, cooling rates, and heating rates on the subsequent melting behavior of PHB were studied in detail. It is found that increasing the MWCNTs loadings, decreasing the cooling rates, and increasing the heating rates would restrict the occurrence of the recrystallization of PHB in the nanocomposites.

© 2009 Wiley Periodicals, Inc. *J Polym Sci Part B: Polym Phys* 47: 2238–2246, 2009

Keywords: biodegradable; biodegradable polymer; crystallization; melting behavior; nanocomposites; nonisothermal melt crystallization; polymer nanocomposites

INTRODUCTION

Biodegradable polymers have received considerable attention in the last 2 decades. Among them, poly(hydroxybutyrate) (PHB) is one of the most extensively studied biodegradable thermoplastic polymers. PHB is a truly biodegradable and biocompatible polymer with relatively high melting point (ca. 180 °C) and crystallinity (>50%).¹ However, practical application of PHB has often been limited by its brittleness and narrow processing window. Therefore,

polymer blending and nanocomposites preparation have often been used for its wide practical application.

Miscible blends have been prepared by mixing PHB with poly(vinyl acetate) (PVAc), poly(epichlorohydrin) (PECH), poly(vinyl phenol) (PVPh), poly(vinylidene fluoride) (PVDF), poly(vinylidene chloride-co-acrylonitrile) (PVDCAN), and poly(ethylene oxide) (PEO).^{2–7} On the other hand, PHB is immiscible with poly(ϵ -caprolactone) (PCL), poly(cyclohexyl methacrylate) (PCHMA), poly(hydroxyoctanoate) (PHO), high-molecular-weight poly(L-lactide) (PLLA), poly(methylene oxide) (PMO), and poly(butylene succinate) (PBSU).^{8–13} Recently, Di Lorenzo et al. and Ha and Cho have reviewed the miscibility, properties, and biodegradability of blends containing PHB

Correspondence to: Z. Qiu (E-mail: qiuzb@mail.buct.edu.cn)

Journal of Polymer Science: Part B: Polymer Physics, Vol. 47, 2238–2246 (2009)
© 2009 Wiley Periodicals, Inc.

and poly(3-hydroxybutyrate-co-hydroxyvalerate) (PHBV), respectively.^{14,15}

Compared with polymer blends, only few works have been reported on the preparation, characterization, crystallization, and properties of PHB-based polymer nanocomposites.^{16–20} The nanofillers used for the preparation of PHB-based nanocomposites are clay and carbon nanotubes (CNTs). PHB/clay nanocomposites usually form intercalated hybrids and show significant improvement in thermal and mechanical properties of the matrix when compared with that of the neat polymer. The amount of silicate and the nature of organic modifier play a dominant role in determining the extent of intercalation in PHB/clay nanocomposites. The crystallization of PHB is accelerated in the nanocomposites because clay particles act as a strong nucleating agent; furthermore, the rate of biodegradation of PHB is enhanced dramatically in the nanohybrids when compared with that of the neat polymer.^{16–19} Recently, PHB/single-walled carbon nanotubes (SWCNTs) nanocomposites have been prepared by solution casting method using chloroform as cosolvent. The crystalline size substantially decreased for the PHB/SWCNTs nanocomposite with a 1% weight fraction of SWCNTs when compared with that of the neat PHB; moreover, the polymer nanocomposite films showed an increase in hardness and Young's modulus with increasing SWCNTs contents.²⁰

However, to the best of our knowledge, biodegradable PHB/multiwalled carbon nanotubes (MWCNTs) nanocomposites have not been reported so far in the literature. Recently, we have prepared PHB/MWCNTs nanocomposites at different MWCNTs loadings and studied the morphology, isothermal crystallization kinetics, and thermal properties by various techniques.²¹ It is found that the crystallization of PHB has been enhanced in the presence of MWCNTs due to the heterogeneous nucleation effect; furthermore, the thermal stability of PHB/MWCNTs has also been improved.

It is of great importance and interest to study the crystallization behavior of biodegradable polymers because it affects not only the crystalline structure and morphology of semicrystalline polymers but also the final physical properties and biodegradability. Therefore, in this work, nonisothermal melt crystallization of neat PHB and its nanocomposites at different MWCNTs loadings was investigated from the viewpoint of practical application because most polymer processing

operations are carried out under nonisothermal conditions. Moreover, subsequent melting behavior of neat PHB and its nanocomposites was also studied to get a better understanding the effect of the presence of MWCNTs and the loadings on the multiple melting behavior of PHB in the nanocomposites crystallized nonisothermally from the melt.

EXPERIMENTAL

PHB ($M_w \approx 2.0 \times 10^5$) was kindly supplied by Biomer Company, Germany. The carboxyl-functionalized multiwalled carbon nanotubes (f-MWCNTs) samples were purchased from Chengdu Institute of Organic Chemistry, Chinese Academy of Sciences. The outer diameter is around 30–50 nm, with lengths ranging between 10 and 20 μm . The PHB/f-MWCNTs nanocomposites were prepared through a solution mixing method. For the fabrication of nanocomposites, PHB was mixed with the addition of various f-MWCNTs contents, specified as 0.5, 1, and 2 wt % in the polymer matrix, respectively. Chloroform was used as the mutual solvent. On one hand, the appropriate amount of f-MWCNTs was added into chloroform. Then, the mixture was sonicated with a KQ 3200E ultrasonic generator at 150 W for 1 h to make a uniformly dispersed suspension. On the other hand, PHB was placed into chloroform at an elevated temperature and stirred for 1 h to dissolve PHB completely. Next, the PHB solution was added to the f-MWCNTs suspension, and sonication was continued at 150 W, with stirring for 6 h. The PHB/f-MWCNTs solution was poured into a dish to evaporate the solvent at room temperature. In the case of neat PHB, it was dissolved into chloroform at 60 °C for 2 h and then cast on a Petri dish. All the samples were further dried at 70 °C under vacuum for 3 days to remove the solvent completely. In this work, neat PHB and its three PHB/f-MWCNTs nanocomposites were abbreviated as 100/0, 99.5/0.5, 99/1, and 98/2, respectively, with the first number referring to PHB, whereas the second number referring to f-MWCNTs.

A field emission scanning electron microscopy (S-4700, Hitachi) was used to observe the morphology of the surfaces of PHB/f-MWCNTs nanocomposites, which were fractured in liquid nitrogen. All specimens were coated with gold before examination. A Hitachi H-800 transmission electron microscopy (TEM) was also used to

investigate the dispersion of f-MWCNTs in the PHB matrix. Thin sections (with thickness of about 50–70 nm) of the nanocomposites were prepared under cryogenic conditions ($-80\text{ }^{\circ}\text{C}$) using a Leica EM FC6 ultramicrotome.

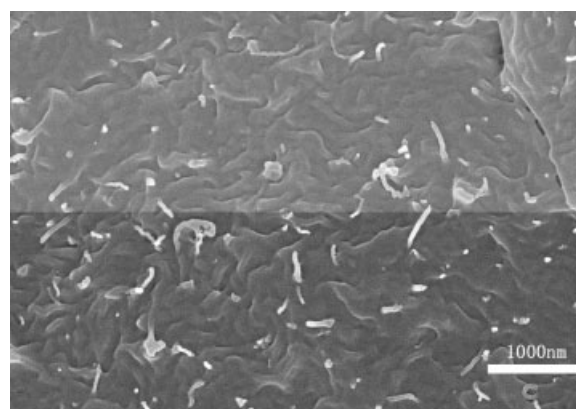
Nonisothermal melt crystallization and subsequent melting behavior of neat PHB and its nanocomposites at different f-MWCNTs loadings were carried out using a TA Instrument differential scanning calorimetry (DSC) Q100 with a Universal Analysis 2000. The samples were first melted at $190\text{ }^{\circ}\text{C}$ for 3 min to erase any thermal history of the samples and cooled to $20\text{ }^{\circ}\text{C}$ at various constant cooling rates ranging from 5 to $25\text{ }^{\circ}\text{C}/\text{min}$. The samples were then heated to the melt again to study the subsequent melting behavior at a heating rate of $20\text{ }^{\circ}\text{C}/\text{min}$ (if not otherwise specified).

RESULTS AND DISCUSSION

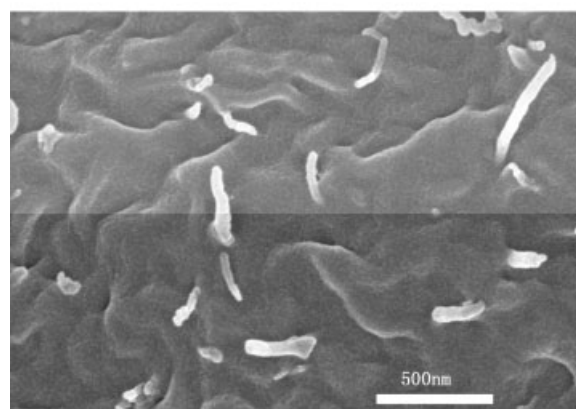
Dispersion of f-MWCNTs in the PHB Matrix

It is well known that the dispersion of CNTs in the polymer matrix must influence the physical properties of polymer matrix. To improve the mechanical, electrical, and thermal performances of the polymer matrix, a fine dispersion of CNTs in the polymer matrix is usually required. Therefore, SEM was used to observe the surfaces of PHB/f-MWCNTs nanocomposites fractured in liquid nitrogen for investigating the dispersion of f-MWCNTs in the PHB matrix. Figure 1(a,b) shows an overview on the fracture surface of a 98/2 nanocomposite at low and high magnification, respectively. Bright dots and lines are the ends of the broken f-MWCNTs, indicative of a homogeneous dispersion of f-MWCNTs in the PHB matrix. Moreover, the ends of individual f-MWCNTs embedded in the matrix can even be observed as some nanotubes seem to be pulled out of the section surface. The homogeneous dispersion of f-MWCNTs has also been found for the 99.5/0.5 and 99/1 samples. No severe aggregation of f-MWCNTs is found in the PHB matrix despite the f-MWCNTs loadings, indicating that the variation of f-MWCNTs contents from 0.5 to 2 wt % does not influence the dispersion and distribution of f-MWCNTs in the polymer matrix significantly.

Figure 1(c) demonstrates the TEM image of the ultrathin section of a 98/2 nanocomposite. It is obvious from Figure 1(c) that f-MWCNTs are randomly dispersed in the PHB matrix without any apparent aggregation. Meanwhile, it can even be



(a)



(b)



(c)

Figure 1. (a) SEM image of fracture surface for a 98/2 nanocomposite at low magnification, (b) SEM image of fracture surface for a 98/2 nanocomposite at high magnification, and (c) TEM image of a 98/2 nanocomposite.

observed that most f-MWCNTs remain curved in shape or even interwoven in the nanocomposite because of the extreme flexibility of the nanotubes. Both SEM and TEM observations suggest a homogeneous distribution of f-MWCNTs in the PHB matrix, which is probably due to the presence of carboxyl group of MWCNTs.

Nonisothermal Melt Crystallization of Neat PHB and PHB/MWCNTs Nanocomposites at Different f-MWCNTs Loadings

As described in the experimental section, nonisothermal melt crystallization of neat PHB and its nanocomposites at different f-MWCNTs loadings was studied with DSC at various cooling rates ranging from 5 to 25 °C/min.

It is of great interest to investigate the presence of f-MWCNTs and their loadings on the nonisothermal melt crystallization of PHB in the nanocomposites. Figure 2 shows the DSC cooling traces of neat PHB and its three nanocomposites at 10 °C/min from the crystal-free melt as an example. Neat PHB has a crystallization peak temperature (T_p) at around 98.5 °C, which shifts to high temperature range in the presence of f-MWCNTs. In the case of 99.5/0.5 and 99/1 samples, T_p s shift to around 101.3 and 102.7 °C, respectively; however, in the case of 98/2 sample, T_p shifts to around 108.2 °C. It is obvious that T_p s of the nanocomposites are always higher than that of the neat PHB at the same cooling rate, indicating that the presence of f-MWCNTs plays a dominant role in accelerating the crystallization of PHB due to the heterogeneous nucleation effect in the nanocomposites. Thus, it can be concluded that the presence of f-MWCNTs enhances the nonisothermal melt crystallization of PHB in the nanocomposites with respect to neat PHB; furthermore, the enhancement is affected significantly by the f-MWCNTs contents. Similar results were also found in other MWCNTs-based nanocomposites with PHBV, PLLA, and isotactic polypropylene (i-PP) being polymer matrix.^{22–24} The effect of f-MWCNTs loadings on the enhancement of nonisothermal melt crystallization of PHB is not significant if the f-MWCNTs loadings are less than 1 wt %; however, such enhancement effect becomes very significant for the PHB/f-MWCNTs nanocomposite containing 2 wt % f-MWCNTs.

It is also well known that the nonisothermal melt crystallization of semicrystalline polymers must also be influenced by the cooling rates. Therefore, in this work, the effect of cooling rates

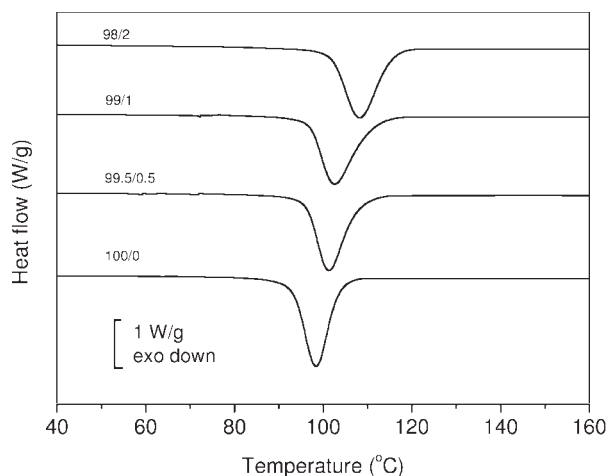


Figure 2. DSC cooling traces of neat PHB and its nanocomposites with different f-MWCNTs loadings at 10 °C/min.

on the nonisothermal melt crystallization of neat PHB and the PHB/f-MWCNTs nanocomposites was further studied. Figure 3(a,b) displays the DSC cooling traces of neat PHB and the 99/1 nanocomposite crystallized nonisothermally from the melt at different cooling rates, respectively. For both neat PHB and the nanocomposite, the crystallization exotherms shift to low temperature range with increasing cooling rate. For neat PHB, T_p is around 101.4 °C at a cooling rate of 5 °C/min, shifting to low temperature range with the increase of cooling rate. At a cooling rate of 25 °C/min, T_p of neat PHB is found to be around 91.9 °C. For the 99/1 nanocomposite, T_p is around 113.4 °C at a cooling rate of 5 °C/min. Similar to neat PHB, T_p s of the 99/1 nanocomposite shift to low temperature range with increasing the cooling rates, too. For instance, T_p of the 99/1 nanocomposite decreases to be around 96.2 °C at a cooling rate of 25 °C/min. Moreover, it can be seen that the difference in T_p s between neat PHB and the nanocomposite is particularly significant at low cooling rates. As mentioned earlier, the difference in T_p s between neat PHB and the 99/1 nanocomposite is around 10 °C at a low cooling rate of 5 °C/min; however, the difference decreases to be only 4.3 °C at a high cooling rate of 25 °C/min. In brief, the aforementioned results suggest that the nonisothermal melt crystallization of PHB/f-MWCNTs nanocomposite is affected not only by the presence of f-MWCNTs but also by the cooling rate.

Figure 4 summarizes the variation of T_p with f-MWCNTs loadings for neat PHB and its three nanocomposites at different cooling rates. The

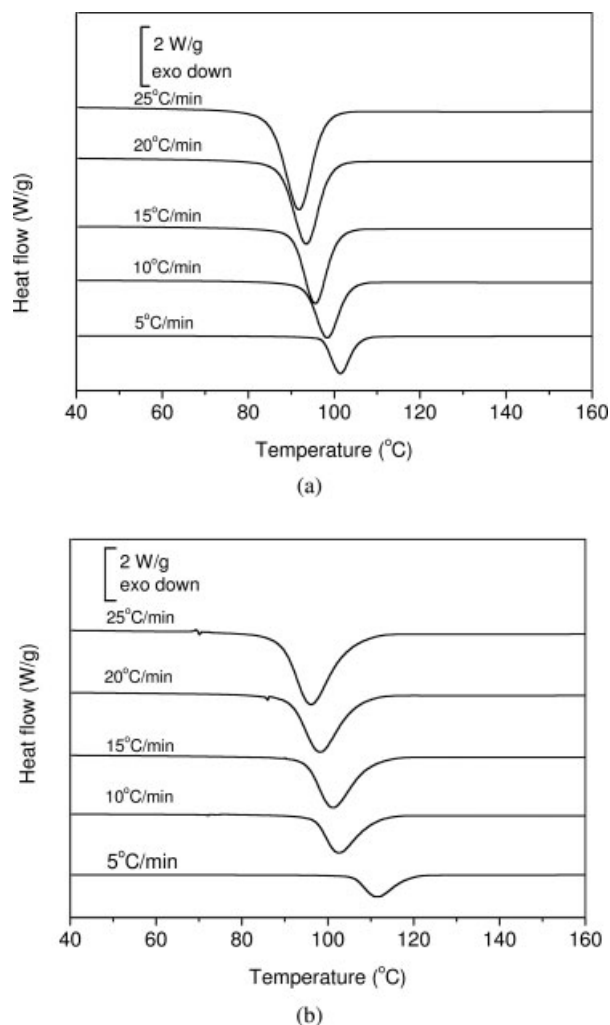


Figure 3. DSC cooling traces of neat PHB and its nanocomposite at indicated cooling rates; (a) neat PHB and (b) 99/1 nanocomposite.

effects of both cooling rates and f-MWCNTs loadings on the variation of T_p can be obtained clearly from Figure 4 for both neat PHB and the PHB/f-MWCNTs nanocomposites at different f-MWCNTs loadings. On one hand, T_p shifts to low temperature range with increasing cooling rate for both neat PHB and its three nanocomposites irrespective of the f-MWCNTs loadings. The samples do not have enough time to crystallize at high temperature range with increasing cooling rate; therefore, the crystallization exotherms shift to low temperature range. On the other hand, T_p s of PHB are always higher in the nanocomposites than in neat PHB at a given cooling rate. T_p s becomes higher with increasing the f-MWCNTs loadings in the nanocomposites, indicating that the nonisothermal melt crystallization of PHB is

enhanced by the presence of f-MWCNTs, and the degree of enhancement in T_p is affected by the f-MWCNTs loadings.

It should be noted that the variation of T_p s is only around 3 °C for neat PHB with decreasing cooling rate from 10 to 5 °C/min; however, the variations of T_p s are around 9 °C for the PHB/f-MWCNTs nanocomposites despite the f-MWCNTs loadings under the same crystallization condition. For the nonisothermal melt crystallization at the cooling rates faster than 10 °C/min, the difference in T_p s is comparable for neat PHB and the PHB/f-MWCNTs nanocomposites with changing the cooling rates. The aforementioned results suggest that the heterogeneous nucleation effect induced by the presence of f-MWCNTs is more pronounced at low cooling rates slower than 10 °C/min during the nonisothermal melt crystallization. From Figure 4, it is obvious that the presence of f-MWCNTs can still enhance the nonisothermal melt crystallization at high cooling rates faster than 10 °C/min; however, the nucleation effect induced by the presence of f-MWCNTs becomes less pronounced. The fact that the nucleation effect becomes less pronounced at fast cooling rates may suggest that the crystal growth rate becomes a limiting factor at higher cooling rates because of restriction of polymer chain mobility.²⁴ Thus, it seems that the cooling rates play a dominant role in influencing the nonisothermal melt crystallization of PHB in the PHB/f-MWCNTs nanocomposites at faster cooling rates. In other words, the nucleation effect induced by the presence of f-MWCNTs is especially pronounced at slow cooling rates, but is masked by restricted crystal growth in the PHB/f-MWCNTs nanocomposites at fast cooling rates, hence suggesting

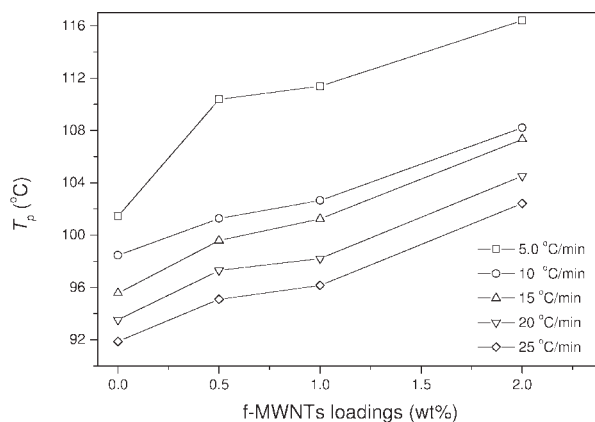


Figure 4. Variation of crystallization peak temperature with f-MWCNTs loadings for neat PHB and its nanocomposites at different cooling rates.

mobility restriction. Miltner et al. also found similar results in the i-PP/MWCNTs nanocomposites.²⁴ Therefore, it can be concluded that nonisothermal melt crystallization of PHB/f-MWCNTs nanocomposites is influenced by both cooling rates and the presence of f-MWCNTs as well as their loadings.

Subsequent Melting Behavior of Neat PHB and PHB/MWCNTs Nanocomposites Crystallized Nonisothermally from the Melt

Double or multiple melting endotherms are often found in semicrystalline polymers crystallized isothermally from the melt at selective crystallization temperature.^{25–30} Liu and Petermann have recently summarized the possible origin of the double or multiple melting endotherms as follows: (1) melting, recrystallization, and remelting during the DSC heating process, (2) the presence of more than one crystal modifications (polymorphism), (3) variation in morphology (such as lamellar thickness, distribution, perfection, or stability), (4) physical aging or/and relaxation of the rigid amorphous fraction, and (5) different molecular weight species and so on.³¹ On the contrary, few works have dealt with the double or multiple melting endotherms of polymers crystallized nonisothermally from the melt at constant cooling rates.^{32–34} However, much more attention should be directed to the nonisothermal melt crystallization and subsequent melting behavior of polymeric materials from the viewpoint of practical application because most semicrystalline polymers are usually processed nonisothermally from the melt.

As introduced in the experimental section, subsequent melting behavior of neat PHB and the PHB/f-MWCNTs nanocomposites was investigated in this work after crystallizing nonisothermally at constant cooling rates from the melt. Effects of the f-MWCNTs loadings, cooling rates, and heating rates on the subsequent melting behavior of PHB were investigated in detail.

The effect of f-MWCNTs loadings on the subsequent melting behavior of neat PHB and its nanocomposites was investigated first by DSC. Figure 5 shows the DSC heating traces of neat PHB and the PHB/f-MWCNTs nanocomposites at 20 °C/min after crystallizing nonisothermally from the melt at a cooling rate of 10 °C/min. As shown in Figure 5, two melting endothermic peaks are observed for both neat PHB and the PHB/f-MWCNTs nanocomposites, which are labeled as T_{m1} and T_{m2} in

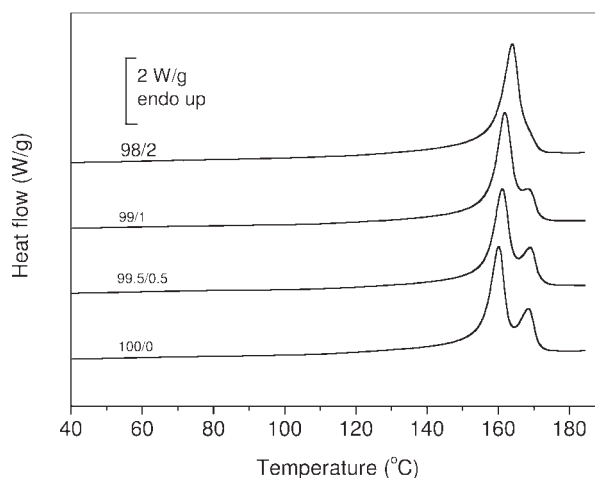


Figure 5. Subsequent melting behavior of neat PHB and its nanocomposites cooled from the melt at 10 °C/min. The heating rate is 20 °C/min.

the order of temperature from low to high. For neat PHB, T_{m1} is around 160.2 °C and T_{m2} is around 168.4 °C. In the PHB/f-MWCNTs nanocomposites, T_{m1} shifts slightly to high temperature with increasing the f-MWCNTs loadings. For instance, T_{m1} s become 161.3, 161.9, and 163.9 °C for the PHB/f-MWCNTs nanocomposites at 0.5, 1, and 2% f-MWCNTs loadings, respectively. The upward shift of T_{m1} may be related to the fact that the corresponding crystal lamellae become thicker with increasing the f-MWCNTs loadings because they were formed at higher temperature during cooling from the melt. On the contrary, T_{m2} shifts slightly to low temperature with increasing the f-MWCNTs loadings in the PHB/f-MWCNTs nanocomposites. For example, T_{m2} is around 170.4 °C for neat PHB, which shifts to be around 169.1 and 168.4 °C, respectively, for the nanocomposites at 0.5 and 1% f-MWCNTs loadings. In the case of the 98/2 nanocomposite, it is hard to observe T_{m2} because it is significantly suppressed and overlapped with T_{m1} . Moreover, T_{m1} increases gradually in area, whereas T_{m2} diminishes gradually with increasing the f-MWCNTs loadings in the PHB/f-MWCNTs nanocomposites, resulting in that the magnitude of the T_{m1} relative to that of the T_{m2} becomes larger.

As shown in Figure 5, neat PHB and PHB/f-MWCNTs nanocomposites show double melting behavior after crystallizing nonisothermally from the melt at a cooling rate of 10 °C/min. Such double melting behavior may be explained by the melting, recrystallization, and remelting model. T_{m1} corresponds to the melting of the crystals formed during the nonisothermal crystallization

from the melt at a constant cooling rate, whereas T_{m2} corresponds to the melting of the crystals formed through recrystallization and reorganization of the crystals of T_{m1} during the subsequent DSC heating scans.^{24,35}

According to the melting, recrystallization, and remelting model, double melting curves observed by DSC are the superposition of three contributions, that is, an endotherm associated with the melting of the original crystals formed before the DSC scan, an exotherm corresponding to recrystallization following the initial melting, and an endotherm associated with the melting of crystals formed by recrystallization. The scanning rate dependence on the multiple melting behavior is often regarded as the evidence of the melting–recrystallization model. To verify the melting and recrystallization mechanism, we studied the heating rate dependence of melting behavior of neat PHB and its nanocomposites. Figure 6(a,b) shows the scanning rate dependence of the melting behavior of neat PHB and the 99/1 nanocomposite crystallized nonisothermally from the melt at a cooling rate of 10 °C/min, respectively. At the heating rates not higher than 10 °C/min, two melting endotherms and one crystallization exotherm are found for the subsequent melting behavior of neat PHB. Furthermore, the shape of the two melting endotherms is found to vary with the heating rate. The magnitude of T_{m1} in area relative to that of T_{m2} becomes larger with increasing heating rate, indicating that the recrystallization of PHB is restricted with increasing heating rate because the time for PHB to melt and recrystallize becomes shorter during the heating process. Finally, T_{m2} becomes a shoulder next to the main melting endothermic peak T_{m1} as the heating rate of 40 °C/min is used. For the 99/1 nanocomposite, it shows the similar subsequent melting behavior as neat PHB. It should be noted that the crystallization exotherm between the two melting endotherms can only be found at slow heating rates of 2.5 and 5 °C/min, respectively. When the heating rate is faster than 10 °C/min, both the two melting endotherms are observed for the subsequent melting behavior of the 99/1 nanocomposite, whereas the exothermic contribution is masked and overlapped by both endothermic ones; thus, crystallization exotherm is not found during the DSC heating scan. As the heating rate of 40 °C/min is used, T_{m2} is heavily suppressed because of restricted mobility and becomes a shoulder next to T_{m1} . It is also interesting to discuss the effect of f-MWCNTs on the mo-

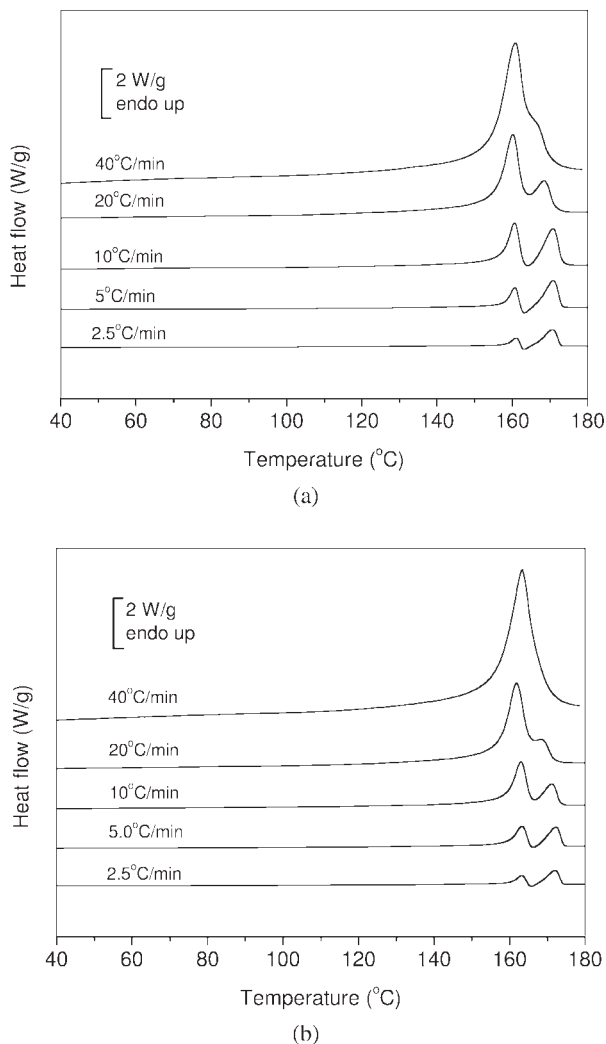


Figure 6. Effect of heating rates on the subsequent melting behavior of neat PHB and its nanocomposite cooled from the melt at 10 °C/min; (a) neat PHB and (b) 99/1 nanocomposite. The heating rates are shown in the figure.

bility and multiple melting behavior of PHB in the PHB/f-MWCNTs nanocomposites. The mobility of PHB is reduced in the PHB/f-MWCNTs nanocomposites because polymer chain diffusion constraints become more significant in a geometrically confined space with increasing the f-MWCNTs loading. The reduced mobility further inhibits the occurrence of recrystallization of PHB in the PHB/f-MWCNTs nanocomposites at higher f-MWCNTs loadings.²⁴ In conclusion, the subsequent melting behavior of neat PHB and the PHB/f-MWCNTs nanocomposites is convincingly explained on the basis of melting, recrystallization, and remelting model.

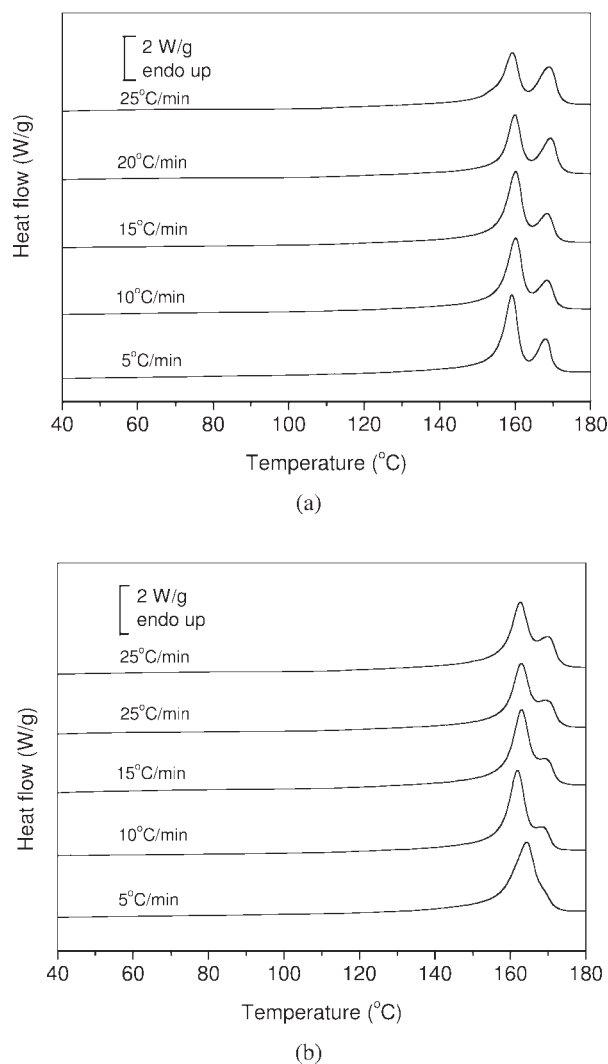


Figure 7. Subsequent melting behavior of neat PHB and its nanocomposite after cooling from the melt at indicated cooling rates; (a) neat PHB and (b) 99/1 nanocomposite. The heating rate is 20 °C/min.

In addition, the effect of cooling rates on the subsequent melting behavior of neat PHB and its nanocomposites was also investigated in this work. Figure 7(a,b) illustrates the DSC heating traces at 20 °C/min for neat PHB and the 99/1 nanocomposite, respectively, crystallized nonisothermally from the melt at the cooling rates ranging from 5 to 25 °C/min. As shown in Figure 7, two melting endothermic peaks are observed for both neat PHB and the 99/1 nanocomposite, respectively. For neat PHB, T_{m1} is around 160 °C, whereas T_{m2} is 169 °C. Furthermore, it is clear that T_{m1} is the major endothermic melting peak compared with T_{m2} despite the cooling rates used. With increasing cooling rate, the shape of the two

melting endotherms is found to vary. The magnitude of T_{m2} in area relative to that of T_{m1} becomes larger with increasing cooling rate, indicating that the recrystallization of PHB is enhanced with increasing cooling rate. The aforementioned results are reasonable because the time for PHB to crystallize becomes shorter with increasing cooling rate; thus, the crystals formed during the nonisothermal melt crystallization are not so perfect and stable, such that they will recrystallize and reorganize into more perfect and stable crystals during the subsequent heating scans. Therefore, T_{m2} becomes more obvious when the high cooling rates are used. In case of the 99/1 nanocomposite, it shows the similar double melting behavior as in neat PHB. T_{m1} is around 163 °C and T_{m2} is around 169 °C. Under the same condition, T_{m2} seems not so obvious in the nanocomposite than in neat PHB, indicating that the presence of f-MWCNTs may restrict the recrystallization of PHB in the nanocomposites compared with that of the neat PHB. The restricted recrystallization of PHB in the nanocomposites may be explained as follows. The presence of f-MWCNTs plays a strong heterogeneous nucleation role in influencing the nonisothermal melt crystallization of PHB in the nanocomposites, resulting in that the nonisothermal melt crystallization of PHB has been enhanced significantly. Therefore, the crystals for the nanocomposites are more perfect and stable than those for neat PHB when the same cooling rate is used; thus, T_{m1} should be higher in the nanocomposites than in neat PHB.²⁴ Accordingly, during the subsequent heating scans, it is easier for neat PHB to recrystallize because of the unstable crystals. On the other hand, it is more difficult for PHB in the nanocomposites to recrystallize because the crystals are more stable and perfect than those in neat PHB. In addition, it should also be noted that the increased mobility restriction is an important factor in hampering the recrystallization of PHB in the PHB/f-MWCNTs nanocomposites as discussed in the previous section.

CONCLUSIONS

In this work, nonisothermal melt crystallization and subsequent melting behavior of neat PHB and PHB/f-MWCNTs nanocomposites at different f-MWCNTs loadings were investigated in detail. It is found that increasing cooling rates shift the crystallization exotherms to low temperature

range for both neat PHB and its nanocomposites. The presence of f-MWCNTs plays an important role in enhancing the nonisothermal melt crystallization of PHB in the nanocomposites due to the heterogeneous nucleation effect; moreover, nonisothermal melt crystallization shifts to high temperature range with increasing the f-MWCNTs loadings. Subsequent melting behavior of neat PHB and its nanocomposites at different f-MWCNTs loadings was studied systematically by considering the effects of the f-MWCNTs loadings, cooling rates, and heating rates. In most cases, double melting behavior is found for both neat PHB and its nanocomposites. Based on the melting, recrystallization, and remelting model, subsequent melting behavior of neat PHB and its nanocomposites can be explained very well. In brief, increasing the f-MWCNTs loadings, decreasing the cooling rates, and increasing the heating rates would restrict the occurrence of the recrystallization of PHB in the nanocomposites.

The authors thank Biomer, Germany for kindly providing PHB samples. Part of this work is financially supported by the National Natural Science Foundation, China (Grant Nos. 20974012, 20504004 and 20774013), Program for New Century Excellent Talents in University (NCET-06-0101), Program for Changjiang Scholars and Innovative Research Team in University (IRT0706), and the project of Polymer Chemistry and Physics, Beijing Municipal Commission of Education (XK100100640). The authors thank the reviewers for their critical comments and kind suggestions.

REFERENCES AND NOTES

- Doi, Y. *Microbial Polyesters*; VCH Publishers: New York, 1990.
- Greco, P.; Martuscelli, E. *Polymer* 1989, 30, 1475–1483.
- Finelli, L.; Sarti, B.; Scandola, M. *J Macromol Sci Pure Appl Chem* 1997, A34, 13–33.
- Iriondo, P.; Iruin, J.; Fernandez-Berridi, M. *Macromolecules* 1996, 29, 5605–5610.
- Avella, M.; Martuscelli, E. *Polymer* 1988, 29, 1731–1737.
- Marand, H.; Collins, M. *ACS Polym Prepr* 1990, 31, 552–553.
- Lee, J.; Nakajima, K.; Ikehara, T.; Nishi, T. *J Polym Sci Part B: Polym Phys* 1997, 35, 2645–2652.
- Lisuardi, A.; Schoenberg, M.; Gada, R.; Gross, A.; McCarthy, S. *Polym Mater Sci Eng* 1992, 67, 298–300.
- Lotti, N.; Pizzoli, M.; Ceccorulli, G.; Scandola, M. *Polymer* 1993, 34, 4935–4940.
- Dufresne, A.; Vincendon, M. *Macromolecules* 2000, 33, 2998–3008.
- Blumm, E.; Owem, A. *Polymer* 1995, 36, 4077–4081.
- Avella, M.; Martuscelli, E.; Orsello, G.; Raimo, M.; Pascucci, B. *Polymer* 1997, 38, 6135–6143.
- Qiu, Z.; Ikehara, T.; Nishi, T. *Polymer* 2003, 44, 2503–2508.
- Di Lorenzo, M.; Raimo, M.; Cascone, E.; Martuscelli, E. *J Macromol Sci Phys* 2001, 40, 639–667.
- Ha, C.; Cho, W. *Prog Polym Sci* 2002, 27, 759–809.
- Lim, S.; Hyun, Y.; Lee, C.; Choi, H. *J Mater Sci Lett* 2003, 22, 299–302.
- Sanchez-Garcia, M.; Gimenez, E.; Lagaron, J. *J Appl Polym Sci* 2008, 108, 2787–2801.
- Maiti, P.; Batt, C.; Giannelis, E. *Biomacromolecules* 2007, 8, 3393–3400.
- Bordes, P.; Pollet, E.; Bourbigot, S.; Avérous, L. *Macromol Chem Phys* 2008, 209, 1473–1484.
- Yun, S.; Gadd, G.; Latella, B.; Lo, V.; Russell, R.; Holden, P. *Polym Bull* 2008, 61, 267–275.
- Xu, C.; Qiu, Z., manuscript in preparation.
- Lai, M.; Li, J.; Yang, J.; Liu, J.; Tong, X.; Cheng, H. *Polym Int* 2004, 53, 1479–1484.
- Zhao, Y.; Qiu, Z.; Yang, W. *J Phys Chem B* 2008, 112, 16461–16468.
- Miltner, H. E.; Grossiord, N.; Lu, K.; Loos, J.; Koning, C. E.; Van Mele, B. *Macromolecules* 2008, 41, 5753–5762.
- Yoo, E.; Im, S. *J Polym Sci Part B: Polym Phys* 1999, 37, 1357–1366.
- Qiu, Z.; Ikehara, T.; Nishi, T. *Polymer* 2003, 44, 3095–3099.
- Qiu, Z. *J Appl Polym Sci* 2007, 104, 3637–3641.
- Toda, A.; Tomita, C.; Hikosaka, M.; Saruyama, Y. *Polymer* 1998, 39, 5093–5104.
- Okazaki, I.; Wunderlich, B. *J Polym Sci Part B: Polym Phys* 1996, 34, 2941–2952.
- Chen, H.; Hwang, J.; Chen, C. *Polymer* 1996, 37, 5461–5467.
- Liu, T.; Petermann, J. *Polymer* 2001, 42, 6453–6461.
- Qiu, Z.; Komura, M.; Ikehara, T.; Nishi, T. *Polymer* 2003, 44, 7781–7785.
- An, Y.; Li, L.; Dong, L.; Mo, Z.; Feng, Z. *J Polym Sci Part B: Polym Phys* 1999, 37, 443–450.
- Song, L.; Qiu, Z. *Polym Degrad Stab* 2009, 94, 632–637.
- Rim, P.; Runt, J. *Macromolecules* 1984, 17, 1520–1526.